ELSEVIER

Catalysis Today 49 (1999) 293–302

CATALYSIS TODAY

Hydroisomerization of *n*-hexane over Pt–SAPO-11 and Pt–SAPO-31 molecular sieves

A.K. Sinha*, S. Sivasanker

National Chemical Laboratory, Pune 411 008, India

Abstract

SAPO-11 and SAPO-31, two medium pore molecular sieves, were synthesized from aqueous and non-aqueous (ethylene glycol) media. Their acidities (by TPD of pyridine) and their catalytic activities in the isomerization of *n*-hexane are compared. Samples synthesized from non-aqueous medium possess more acidity and higher activities than those obtained from aqueous medium. ^{29}Si MAS NMR studies suggest greater substitution of P^{5+} by Si^{4+} and lower concentration of silica islands in the samples synthesized from non-aqueous medium. Both SAPO-11 and -31 produce predominantly the monomethyl isomers due to their medium size pores. The activity studies were carried out over Pt-loaded samples in the presence of H_2.

Keywords: Hydroisomerization; Pt–SAPO-11; Pt–SAPO-31

1. Introduction

Hydroisomerization of *n*-paraffins over solid acid catalysts is used to produce high octane gasoline blending components [1], to increase the low temperature performance of diesel [2] and to obtain high viscosity index lube oils [3]. These isomerization reactions are generally carried out over bifunctional catalysts containing metallic sites for hydrogenation/dehydrogenation and acid sites for skeletal isomerization via carbenium ions [4]. The presence of acidic sites and the shape selective features of zeolites [5] has spurred a widespread interest in identifying newer materials such as silicoaluminophosphates based catalysts for the hydroisomerization of paraffinic feedstocks.

Shape selective molecular sieves suppress multibranched isomer formation [6] which are more susceptible to hydrocracking, thereby leading to high isomerization selectivities [7]. SAPO-11, a medium pore silicoaluminophosphate has been used in a selective isomerization process for the manufacture of high viscosity index lube oils from waxes (long chain alkanes) [3]. Parlitz et al. [8] have shown that *n*-heptane undergoes only one branching reaction over SAPO catalysts of various pore sizes so that di- and tribranched isomers are formed only in minor quantities. Campelo et al. [9,10] have suggested that differences in the reaction schemes for *n*-heptane and *n*-hexane transformation over Pt/SAPO-5 and Pt/SAPO-11 arise from differences in their structures. Mériaudeau et al. [11] have found differences in selectivity in the isomerization of *n*-octane over medium pore SAPO-11, SAPO-31 and SAPO-41 and have explained them on the basis of diffusional restrictions and steric constraints.

The present work compares SAPO-11 and SAPO-31 synthesized by two different routes (from aqueous and non-aqueous media) in the isomerization of

*Corresponding author.

0920-5861/99/$ – see front matter
PII: S0920-5861(98)00436-2

n-hexane. Further, studies were carried out using C_7, C_8 and C_{16} *n*-alkanes to study the influence of increasing chain length of the reactant molecules on conversion and product selectivity. SAPO-11 has one-dimensional 10-membered ring channels with an elliptical pore opening of 0.44×0.64 nm. SAPO-31 has circular unidimensional 12-membered ring channels of 0.54 nm diameter.

2. Experimental

SAPO-11(a) and SAPO-31(a) were hydrothermally synthesized from an aqueous medium based on the method described by Lok et al. [12]. SAPO-11(na) and SAPO-31(na) were prepared by a similar procedure, but using the non-aqueous solvent, ethylene glycol. Aluminium isopropoxide (98%, Aldrich), orthophosphoric acid (85%, SD Fine Chem, India), fumed silica and dipropylamine (DPA, Aldrich) were used in the syntheses. The molar gel compositions and crystallization conditions are presented in Table 1 [13]. The compositions used were based on synthesis optimization carried out separately. Earlier workers have also found that different initial gel compositions were necessary for different media to obtain highly crystalline materials [14]. The synthesis products were washed, dried at 393 K for 6 h and calcined at 823 K for 8 h in air by gradually raising the temperature (2 K min^{-1}). Pt was loaded on the SAPOs by wet impregnation with an aqueous solution of $Pt(NH_3)_4Cl_2$ (99%, Aldrich). The resulting materials were dried at 393 K for 4 h and calcined at 823 K for 3 h in air.

The SAPOs were characterized by X-ray powder diffraction (Rigaku Model D/Max-VC, Cu K_α radiation, Ni filter, λ=1.5404 Å) and scanning electron microscopy (JEOL JSM-840 A). Chemical composition was determined by atomic absorption spectroscopy. The acidity of the samples was characterized by chemisorption of pyridine and temperature programmed desorption under chromatographic conditions [15]. ^{29}Si MAS NMR spectra were recorded on a Bruker MSL-300 spectrometer [16].

The hydroconversion of *n*-alkanes was carried out in a fixed bed down flow tubular glass reactor at atmospheric pressure in the temperature range 548–648 K, WHSV (h^{-1}) range 1–4 and H_2/hydrocarbon (mol) ratio between 5 and 20. The catalyst powder was pelletized, sieved to 10–20 mesh size and 2 g of it was loaded into the reactor. Before activity measurements, the catalyst was activated at 648 K in flowing hydrogen (25 ml min^{-1}) for 1 h. The reactants were fed using a syringe pump (Sage instruments, USA). The reaction products were analysed using a Hewlett-Packard gas chromatograph (5880A) with a flame ionization detector and a capillary column (50 m×0.2 mm; HP1, cross linked methyl silicon gum). The isomeric products from *n*-hexadecane reaction were identified by GC–MS.

3. Results and discussion

3.1. Physicochemical characterization

The XRD patterns of SAPO-11(a), -11(na), -31(a), -31(na) were identical to those reported [12]. SEM micrographs revealed similar morphology and average particle size for the samples synthesized from aqueous and non-aqueous media. The physicochemical properties of all the samples are given in Table 2. Based on the TPD studies, the samples can be arranged in the order of decreasing acidity (pyridine desorbed beyond 573 K) as SAPO-31(na)>SAPO-11(na)>SAPO-31(a) >SAPO-11(a) (Table 2). When Si^{4+} is substituted in the $AlPO_4$ framework, it can substitute for P^{5+} ions

Table 1
Synthesis conditions for SAPOs

Sample	Chemical composition (gel)	Conditions		pH (gel)
		Time (h)	Temperature (K)	
SAPO-11(a)	Al_2O_3:1.0 P_2O_5:1.0 DPA: 0.2 SiO_2:50 H_2O	24	473	5.8
SAPO-11(na)	Al_2O_3:1.8 P_2O_5:5.0 DPA: 0.2 SiO_2:60 EG	144	473	6.8
SAPO-31(a)	Al_2O_3:1.1 P_2O_5:1.0 DPA: 0.2 SiO_2:50 H_2O	24	473	6.2
SAPO-31(na)	Al_2O_3:1.8 P_2O_5:5.0 DPA: 0.2 SiO_2:60 EG	72	473	7.0

Table 2
Physicochemical properties of the SAPOs

Catalyst	Chemical composition	Surface area ($m^2\ g^{-1}$)	Partical size (μm)	Pyridine desorbed (μmol g^{-1} catalyst[a])
SAPO-11(a)	$(Al_{0.57}P_{0.38}Si_{0.05})O_2$	140.3	1.5–2.5	59.0
SAPO-11(na)	$(Al_{0.59}P_{0.32}Si_{0.07})O_2$	183.2	2.0	112.0
SAPO-31(a)	$(Al_{0.56}P_{0.41}Si_{0.03})O_2$	207.0	3.5×1.0	69.3
SAPO-31(na)	$(Al_{0.61}P_{0.35}Si_{0.04})O_2$	221.6	2.5×2.0	139.0

[a]Based on pyridine desorbed above 573 K.

leading to a negative charge on the framework (and generation of a Bronsted site when H^+ is picked up) or form SiO_2 islands without generating much acidity [17].

The silicons in the SiO_2 islands can possess different types of first neighbours and the ^{29}Si MAS NMR spectra of SAPOs contain a number of closely spaced lines. The NMR chemical shift of isolated Si ions [Si(4Al)] is around $\delta=-90$ to -95 ppm while it is $\delta=-105$ to -110 ppm for the Si ions inside silica islands [Si(4Si)]. The ^{29}Si MAS NMR spectra of all the four samples had a number of unresolved signals in the chemical shift range of -85 to -115 ppm. However, distinct differences could be observed between the spectra of the samples synthesized from aqueous and non-aqueous media. The samples synthesized from non-aqueous medium exhibited a smaller peak at $\delta=-105$ to -110 ppm (attributed to the non-acidic silica species) than the samples synthesized from aqueous medium suggesting that the concentration of silica 'islands' was less in the former samples. Also, the signal at $\delta=-90$ to -95 ppm (isolated Si ions) is larger in the non-aqueous samples suggesting preferential P^{5+} substitution and generation of larger amounts of Bronsted acidity. The larger concentration of medium acid sites in SAPOs synthesized in non-aqueous media (Table 2) confirms the greater substitution of P^{5+} in the $AlPO_4$ framework by Si^{4+} in the samples synthesized from the non-aqueous medium. Venkatathri et al. [18] had earlier made similar obser-

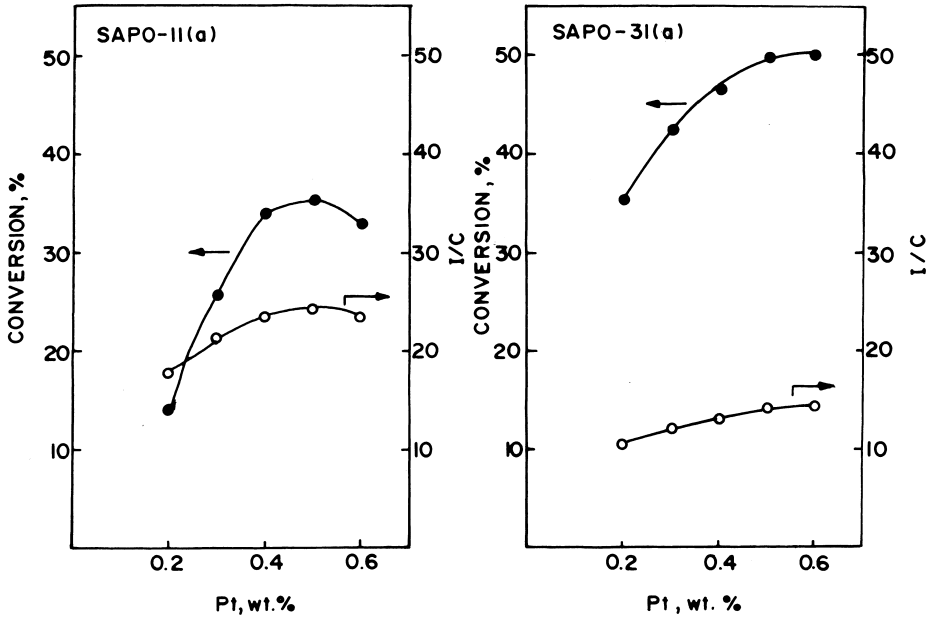

Fig. 1. Influence of Pt content on *n*-hexane isomerization. (Temperature=573 K; WHSV (h^{-1})=1; H_2/*n*-hexane (mol)=5; TOS=1 h.)

vations during studies on the synthesis of SAPO-35 from aqueous and non-aqueous media.

3.2. N-Hexane isomerization

Catalytic hydroconversion of *n*-hexane involves the initial dehydrogenation of *n*-hexane to *n*-hexene on metallic sites, the subsequent isomerization of *n*-hexenes to isohexenes on acidic sites and their final migration to metallic sites and hydrogenation to isohexanes. In addition, the isohexenes formed may undergo isomerization among themselves or cracking on the acid sites.

3.2.1. Influence of Pt content on n-hexane isomerization

The influence of Pt content on conversion and selectivity to isomerization (expressed as the isomer-

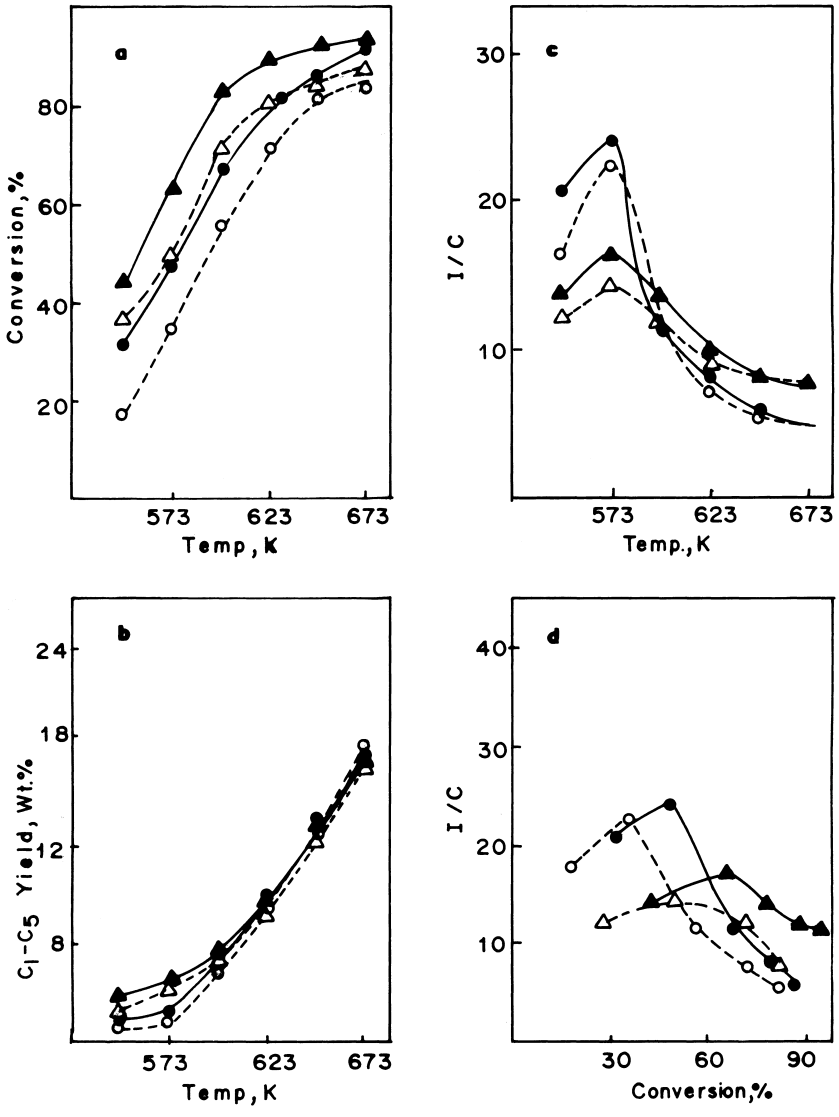

Fig. 2. Influence of temperatue on *n*-hexane isomerization. (WHSV (h^{-1})=1; H_2/*n*-hexane (mol)=5; TOS=1 h.) (○) Pt–SAPO-11(a); (●) Pt–SAPO-11(na); (△) Pt–SAPO-31(a); (▲) Pt–SAPO-31(na).

ization/cracking ratio, I/C) was investigated using SAPO-11(a) and SAPO-31(a). The results obtained at 573 K (WHSV=1 h^{-1} and H_2/*n*-hexane=5 mol) after a TOS (time on stream) of 1 h are presented in Fig. 1. In all the experiments described in this paper, the catalysts generally deactivated slightly with duration of run (TOS), the deactivation being more rapid during the first few minutes. However, the activity became nearly stable after about 45 min and the data collected at a TOS of 1 h are reported. Increasing the Pt content increased both the conversion and I/C ratio until a plateau (or a maximum) was reached at about 0.5 wt% Pt (Fig. 1). This behaviour is typical of bifunctional catalysis [19–21]. The reason for the initial increase in the I/C ratios with increasing Pt content was the greater availability of Pt sites in the vicinity of acid sites enabling rapid hydrogenation of the carbenium ions (and olefins) and desorbing them as alkanes before they underwent cracking reactions.

3.2.2. *Influence of temperature*

The conversion of *n*-hexane increased with temperature over all the four catalysts (Fig. 2(a)). The increase in conversion is less rapid at higher temperatures. This is probably due to diffusion effects at high conversions, besides being also due to more rapid

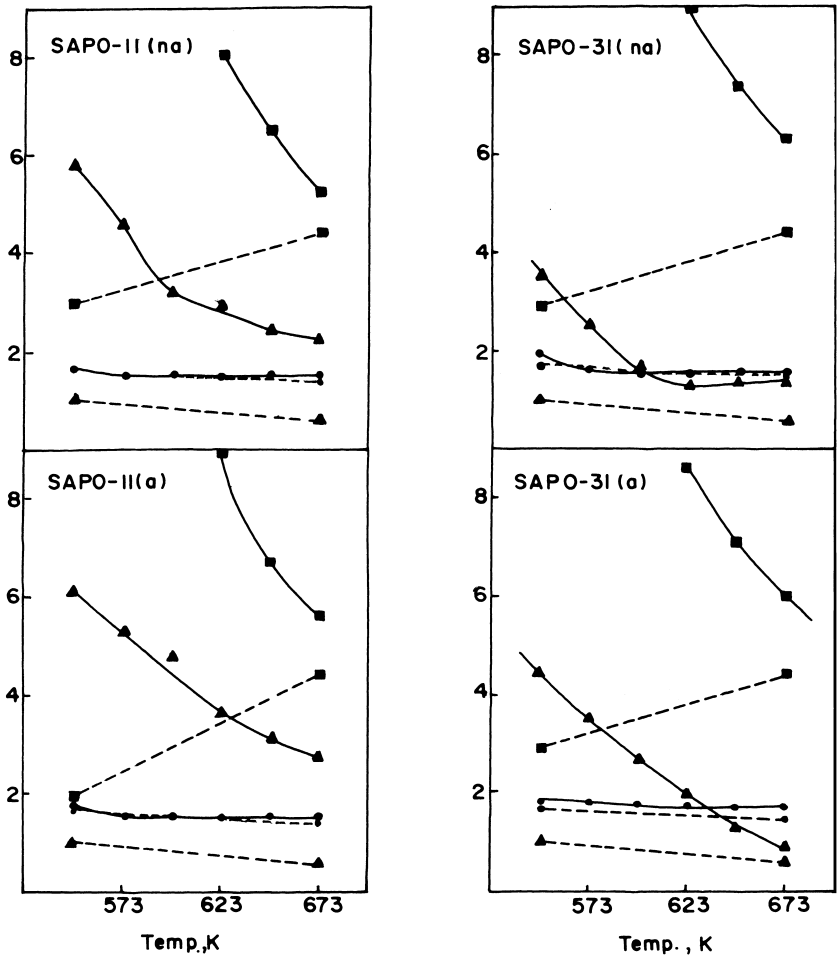

Fig. 3. Influence of temperature on ratios of isomeric hexanes. (WHSV (h^{-1})=1; H_2/*n*-hexane (mol)=5; TOS=1 h.) (●) 2 methyl pentane/3 methyl pentane; (▲) 2,3 dimethyl butane/2,2 dimethyl butane; (■) methyl pentanes/dimethyl butanes; (———) experimental; (- - -) thermodynamic (adapted from [21]).

initial deactivation at higher temperatures; the data reported were collected at a TOS of 1 h. As expected from their higher acidities, SAPOs synthesized from non-aqueous media showed higher conversions. SAPO-31 was more active than SAPO-11 due to the larger number of acid sites in the former (Table 1). Hydroconversion activity decreased as: Pt–SAPO-31(na)>Pt–SAPO-31(a)>Pt–SAPO-11(na)>Pt–SAPO-11(a). Over the SAPO catalysts studied, the yields of the cyclized products (and aromatics) were always small (less than 2% at the highest conversion). Small amounts of olefins were also found in the products. The major products were isohexanes (methyl pentanes and dimethylbutanes) and cracked gases (C_1–C_5) (Fig. 2(b)). It can be assumed that the major production of C_1 and C_2 resulted from *n*-hexane hydrogenolysis along with equimolar amounts of C_4 and C_5. Acid catalysed cracking of 3-methylpentane could have also yielded ethane and butane. Propane was the major cracking product.

A good measure of the performance of the samples as hydroisomerization catalysts can be arrived at from the weight ratios of the isomerized products to the cracked products (I/C); the better catalyst yields products with higher I/C ratios at a specified conversion. The I/C ratios of the products obtained over the four

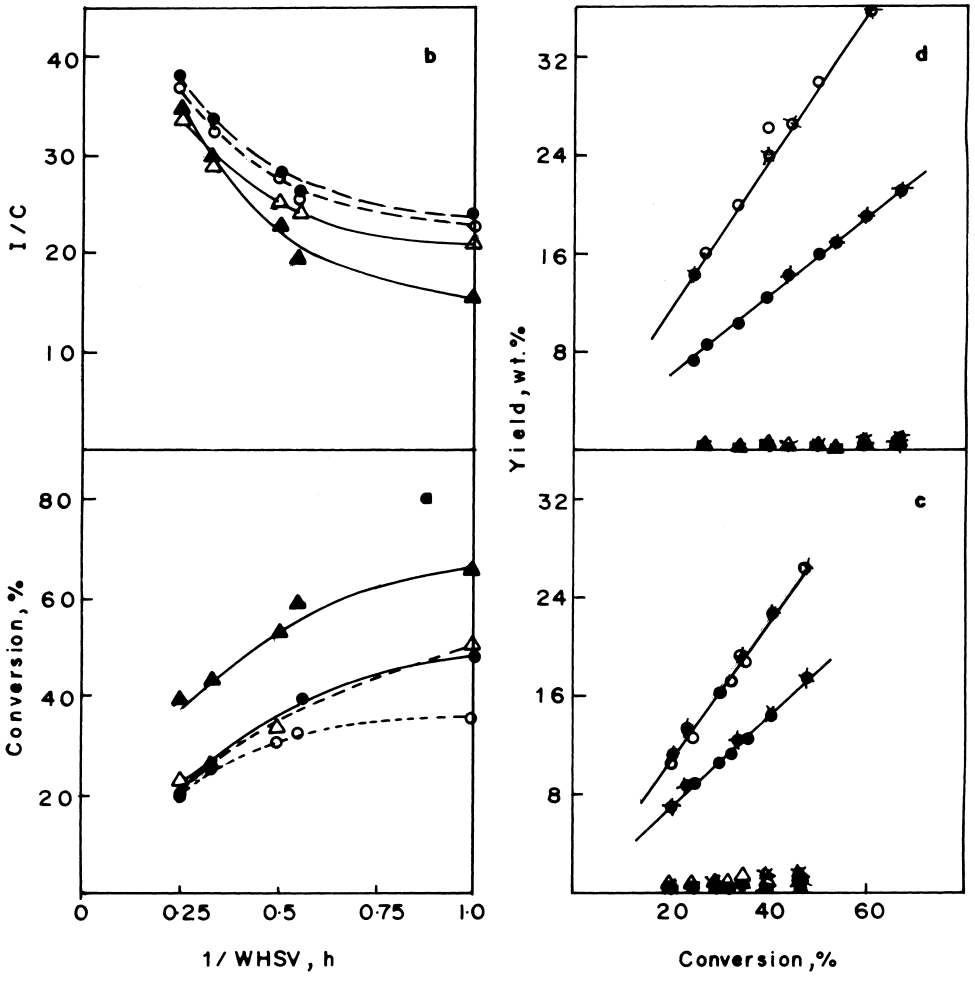

Fig. 4. Influence of space velocity (and conversion) on *n*-hexane isomerization. (Temperature=573 K; H_2/*n*-hexane (mol)=5; TOS=1 h.) a, b; (○) Pt–SAPO-11(a); (●) Pt–SAPO-11(na); (△) Pt–SAPO-31(a); (▲) Pt–SAPO-31(na). c, d: (○) 2 Me-Pentane; (●) 3 Me-Pentane; (△) 2,3 dime-butane; (■) 2, 2 dime-butane; (X) for samples from non-aqueous medium.

catalysts are presented in Fig. 2(c) and (d). The ratios pass through maxima (at ~573 K) with increasing temperature for all the samples. The reason for the maximum is not clear though a possible explanation is that at the intermediate temperature (573 K), the desorption and hydrogenation of the intermediate iso-olefins into isoparaffins is maximum. At lower temperatures, the desorption of the iso-olefin may be slower resulting in greater cracking of the adsorbed species, while at higher temperature, the hydrogenolysis activity of the metal may be more. In general, the samples (na) prepared from non-aqueous media possessed greater isomerization selectivities. The isomerization products obtained were predominantly monobranched over both Pt/SAPO-31 and Pt/SAPO-11 resulting from diffusional limitations in the one-dimensional medium size pores. Only at higher temperatures (high conversions) dimethyl butane formation was substantial. There was a continuous increase in the yields of the isomers, the increase in the dimethylbutanes becoming more rapid at higher temperatures. The breakdown of the components in the isohexane fraction showed that the monobranched isomers decreased while the dibranched isomers increased with increasing temperature suggesting the transformation of the former into the latter compounds. The 2-methyl pentane/3-methyl pentane ratios were in the range of 1.7–1.45 in the temperature range studied, being very close to the thermodynamic equilibrium values (1.65 at 523 K to 1.45 at 673 K; extrapolated from [21]) over all the catalysts (Fig. 3). However, the methylpentanes/dimethylbutanes (MP/DMB) ratios were far from the equilibrium values (Fig. 3). Similarly, the 2,3-dimethyl butane/2,2-dimethyl butane ratios were also far from the equilibrium values. The MP/DMB ratios were farther away from equilibrium values in the case of SAPO-31 than SAPO-11 eventhough the former was more acidic suggesting that the pore dimensions play an important role.

3.2.3. *Influence of space velocity*

An increase in conversion and a decrease in I/C ratio was found with an increase in the contact time (Fig. 4(a) and (b)). The decrease in the I/C ratio is due to an increase in cracking, which being slower than the isomerization reaction is favoured at larger residence times. Besides, at these conditions, larger concentrations of the isomerized products (secondary and tertiary carbo-cations) are present which crack easily. Plots of yields of individual isohexanes as a function of conversion in the case of SAPO-11 and SAPO-31 are presented in Fig. 4(c) and (d), respectively. The plots for 2-methyl and 3-methyl pentane pass through the origin on extrapolation suggesting these to be the primary products of the isomerization reaction. The dimethyl butanes are formed from the subsequent isomerization of the methyl pentanes [21,22]. The yields of dimethyl butanes were more over Pt–SAPO-11 than over Pt–SAPO-31 (Fig. 4(c) and (d)). This is probably due to the elliptical nature of the pores and the slightly larger pore diameter in SAPO-11 (0.64 Å major diameter) enabling the dimethyl butanes (5.6–7.0 Å diameter) to diffuse out of the channels.

The influence of changing in the H_2/n-C_6 (mol) ratio on the conversion and I/C values is presented in Fig. 5. Increasing the H_2/n-C_6 (mol) ratio from 5 to 20 (H_2 partial pressure from 0.83 to 0.95 atm.) decreased conversion and increased I/C ratios. As the studies

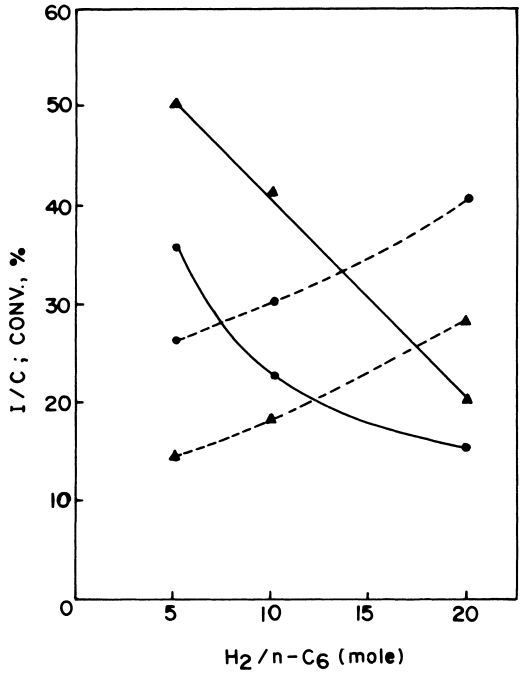

Fig. 5. Influence of H_2/n-C_6 (mol) ratio (at constant feed ratio of *n*-hexane) on conversion and I/C ratios. (Temperature=573 K; WHSV (h^{-1})=1; TOS=1 h.) (●) Pt–SAPO-11(a); (▲) Pt–SAPO-31(a); (———) conversion; (- - -) I/C.

were conducted at a constant feed rate of *n*-hexane (WHSV (h^{-1})=1), the decrease in conversion was probably more due to an increase in the overall (*n*-C_6+H_2) space velocity than due to a negative order w.r.t. H_2 (as reported by earlier workers [23]) especially as the H_2 partial pressures were changed only to a small extent from 0.83 to 0.95 atm. The increase in the I/C ratios is mainly due to lower conversions as the more easily crackable isoalkanes were present in smaller amounts.

3.3. Hydroconversion of long chain alkanes

The conversions of *n*-hexane, *n*-heptane, *n*-octane and *n*-hexadecane at different temperatures over the four catalysts are presented in Fig. 6(a)–(d). As expected, the conversion increased as a function of carbon chain length. However, the increase was much less than expected purely on the basis of chain length. The maximum observed ratio of conversion between *n*-C_{16} and *n*-hexane was only 2.9 (SAPO-11(a) at 548 K), whereas based purely on a carbenium ion mechanism one would have expected much larger ratios (as observed for the cracking of hydrocarbons [24]). Apparently, the larger molecules suffered greater diffusional constraints than the smaller ones. Besides, as already noticed in the case of *n*-hexane, SAPO-31 was more active than SAPO-11 and samples synthesized from non-aqueous medium were more active than the ones from aqueous medium. The I/C ratios of the products obtained over the four catalysts from different alkanes are presented in Fig. 7. While the I/C ratio for *n*-hexane and *n*-heptane hydroconversion passed through a maximum with conversion, for

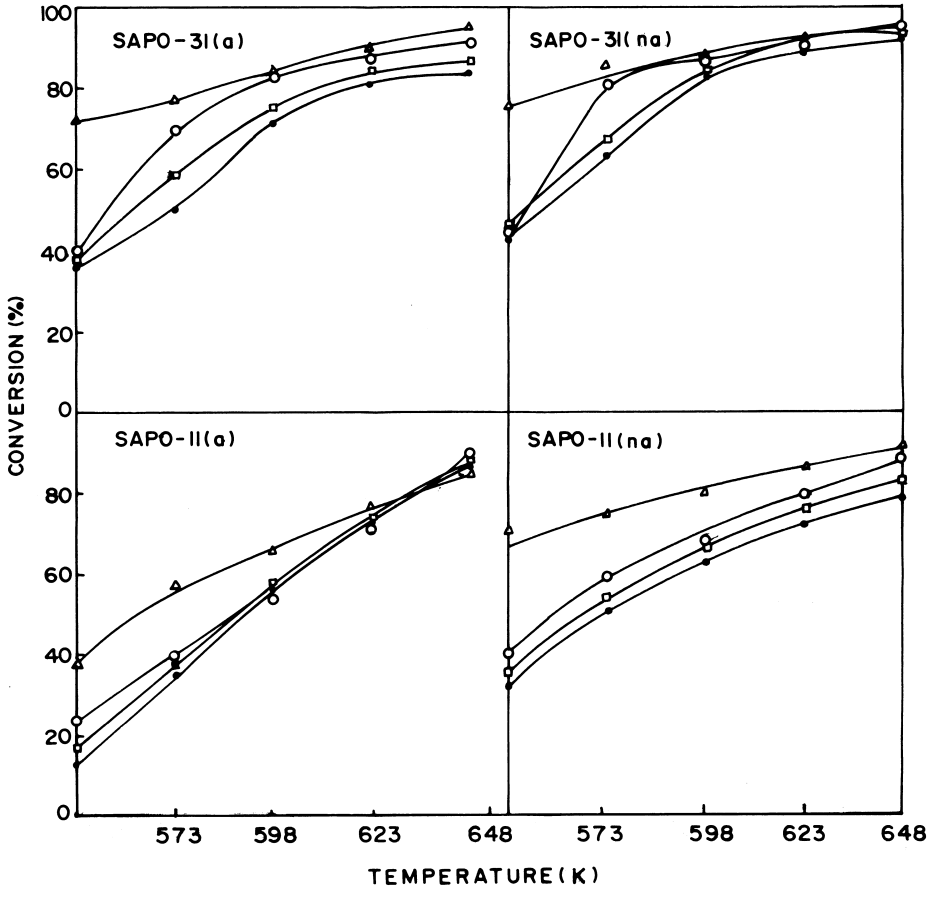

Fig. 6. Influence of temperature on conversion. (WHSV (h^{-1})=1; H_2/*n*-hexane (mol)=5; TOS=1 h.) (●) *n*-hexane; (□) *n*-heptane; (○) *n*-octane; (△) *n*-hexadecane.

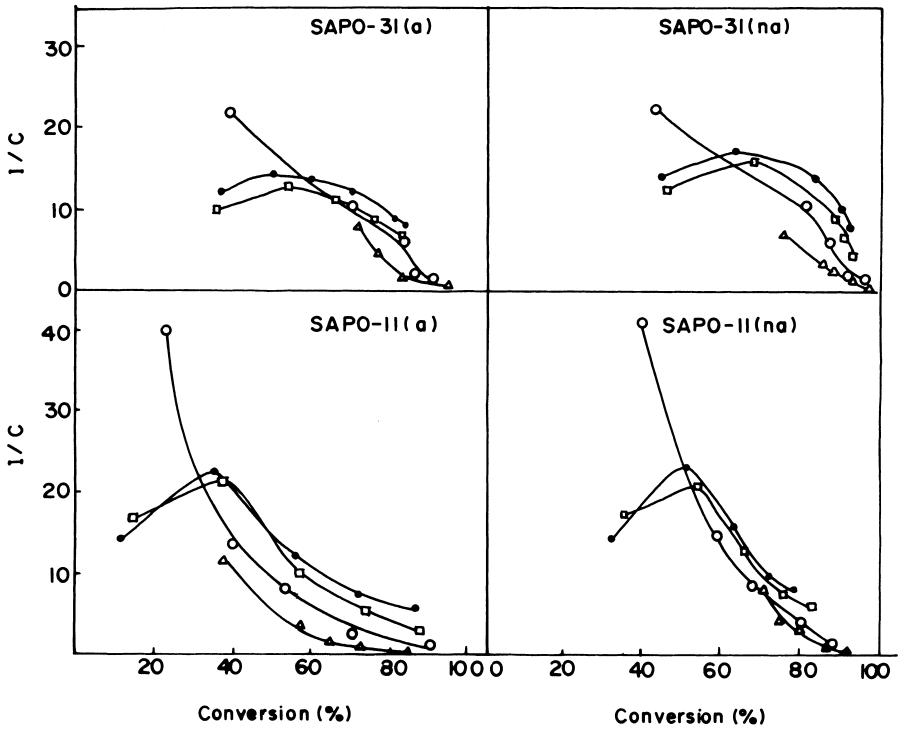

Fig. 7. Ratios of isomerization/cracking yield (I/C) as a function of conversion. (H_2/*n*-hexane (mol)=5; TOS=1 h.) (●) n-hexane; (□) *n*-heptane; (○) *n*-octane; (△) *n*-hexadecane.

n-octane and *n*-hexadecane the I/C ratio decreased monotonously (Fig. 7). It is possible that in the latter cases, the maximum I/C ratio lay at lower conversion levels. In general, the samples prepared from non-aqueous media possessed greater isomerization selectivities.

4. Conclusions

SAPO-11 and SAPO-31 synthesized in ethylene glycol possessed more acidity than those obtained from aqueous media as a result of preferential substitution of P^{5+} ions by Si^{4+}. As a result, they were more active in the hydroisomerization of *n*-hexane. Even though the major isomerization products over both the samples were the monomethyl pentanes, SAPO-11 produced slightly more dimethyl butanes than SAPO-31 due to its slightly larger pore size. Studies on the cracking of larger alkanes (C_7–C_{16}) have suggested the presence of increasing diffusion constraints with increase in the size of the molecule.

Acknowledgements

AKS thanks CSIR, New Delhi, India, for a Senior Research Fellowship.

References

[1] N.A. Cusher, P. Greenouch, J.R.K. Rolfe, J.A. Weiszmann, in: R.A. Meyers (Ed.), Handbook of Petroleum Refining Process, Chapter 5, p. 5, McGraw-Hill, New York, 1986.
[2] S.J. Miller, Stud. Surf. Sci. Catal. 84C (1994) 2319.
[3] S.J. Miller, Microporous Mater. 2 (1994) 439.
[4] G. Giannetto, G. Perot, M.R. Guisnet, Ind. Eng. Prod. Res. Dev. 25 (1986) 481.
[5] S.M. Csicsery, Zeolites 4 (1984) 202.
[6] S. Ernst, J. Weitkamp, J.A. Martens, P.A. Jacobs, Appl. Catal. A 48 (1989) 137.

[7] J.A. Martens, P.A. Jacobs, J. Weitkamp, Appl. Catal. A 20 (1986) 239.
[8] B. Parlitz, E. Schrier, H. Eckelt, C. Lieschke, G. Lieschke, R. Fricks, J. Catal. 155 (1995) 1.
[9] J.M. Campelo, F. Lafont, J.M. Marinas, Zeolites 97 (1995) 15.
[10] J.M. Campelo, F. Lafont, J.M. Marinas, J. Catal. 156 (1995) 11.
[11] P. Mériaudeau, V.A. Tuan, V.T. Nghiem, S.Y. Lai, L.N. Hung, C. Naccache, J. Catal. 160 (1997) 55.
[12] B.M. Lok, C.A. Messina, R.L. Patton, R.T. Gajek, T.R. Cannan, E.M. Flanigen, US Patent 4 40 871 (1984).
[13] A.K. Sinha, S. Sivasanker, P. Ratnasamy, Ind. Eng. Chem. Res. 37 (1998) 2208.
[14] Huo Qisheng, Xu Ruren, J. Chem. Soc., Chem. Comm. (1990) 783.
[15] V.R. Choudhary, V.S. Nayak, Appl. Catal. A 4 (1982) 31.
[16] R. Ravishankar, T. Sen, S. Sivasanker, S. Ganapathy, J. Chem. Soc., Faraday Trans. 91 (1995) 3549.
[17] D. Barthomeuf, Zeolites 14 (1994) 394.
[18] N. Venkatathri, S.G. Hegde, P.R. Rajmohanan, S. Sivasanker, J. Chem. Soc., Faraday Trans. 93 (1997) 3411.
[19] L.J. Leu, L.-Y. Hou, B.-D. Kang, C. Li, S.-T. Wu, J.-C. Wu, Appl. Catal. 69 (1991) 49.
[20] P.B. Weisz, Adv. Catal. 13 (1962) 137.
[21] J.-K. Chen, A.M. Martin, Y.G. Kim, V.T. John, Ind. Eng. Chem. Res. 27 (1988) 401.
[22] G.B. Marin, G.F. Froment, Chem. Eng. Sci. 37(5) (1982) 759.
[23] M. Guisnet, V. Fouche, M. Belloum, J.P. Bournonville, C. Travers, Appl. Catal. 71 (1991) 295.
[24] H.H. Voge, in: P.H. Emmett (Ed.), Catalysis, vol. VI, Reinhold, New York, 1958, p. 407.